

# Comparison of protein expression during wild-type, and E1B-55k-deletion, adenovirus infection using quantitative time-course proteomics

Fu, Yen; Turnell, Andrew; Davis, Simon; Heesom, Kate; Evans, Vanessa; Matthews, David

DOI:

[10.1099/jgv.0.000781](https://doi.org/10.1099/jgv.0.000781)

License:

Creative Commons: Attribution (CC BY)

*Document Version*

Publisher's PDF, also known as Version of record

*Citation for published version (Harvard):*

Fu, Y, Turnell, A, Davis, S, Heesom, K, Evans, V & Matthews, D 2017, 'Comparison of protein expression during wild-type, and E1B-55k-deletion, adenovirus infection using quantitative time-course proteomics', *Journal of General Virology*, vol. 98, no. 6, pp. 1377-1388. <https://doi.org/10.1099/jgv.0.000781>

[Link to publication on Research at Birmingham portal](#)

## General rights

Unless a licence is specified above, all rights (including copyright and moral rights) in this document are retained by the authors and/or the copyright holders. The express permission of the copyright holder must be obtained for any use of this material other than for purposes permitted by law.

- Users may freely distribute the URL that is used to identify this publication.
- Users may download and/or print one copy of the publication from the University of Birmingham research portal for the purpose of private study or non-commercial research.
- User may use extracts from the document in line with the concept of 'fair dealing' under the Copyright, Designs and Patents Act 1988 (?)
- Users may not further distribute the material nor use it for the purposes of commercial gain.

Where a licence is displayed above, please note the terms and conditions of the licence govern your use of this document.

When citing, please reference the published version.

## Take down policy

While the University of Birmingham exercises care and attention in making items available there are rare occasions when an item has been uploaded in error or has been deemed to be commercially or otherwise sensitive.

If you believe that this is the case for this document, please contact [UBIRA@lists.bham.ac.uk](mailto:UBIRA@lists.bham.ac.uk) providing details and we will remove access to the work immediately and investigate.

# Comparison of protein expression during wild-type, and E1B-55k-deletion, adenovirus infection using quantitative time-course proteomics

Yen Rong Fu,<sup>1</sup> Andrew S. Turnell,<sup>2</sup> Simon Davis,<sup>2</sup> Kate J. Heesom,<sup>3</sup> Vanessa C. Evans<sup>1</sup> and David A. Matthews<sup>1,\*</sup>

## Abstract

Adenovirus has evolved strategies to usurp host-cell factors and machinery to facilitate its life cycle, including cell entry, replication, assembly and egress. Adenovirus continues, therefore, to be an important model system for investigating fundamental cellular processes. The role of adenovirus E1B-55k in targeting host-cell proteins that possess antiviral activity for proteasomal degradation is now well established. To expand our understanding of E1B-55k in regulating the levels of host-cell proteins, we performed comparative proteome analysis of wild-type, and E1B-55k-deletion, adenovirus-infected cancer cells. As such we performed quantitative MS/MS analysis to monitor protein expression changes affected by viral E1B-55k. We identified 5937 proteins, and of these, 69 and 58 proteins were down-regulated during wild-type and E1B-55k (*d11520*) adenovirus infection, respectively. This analysis revealed that there are many, previously unidentified, cellular proteins subjected to degradation by adenovirus utilizing pathways independent of E1B-55k expression. Moreover, we found that ALCAM, EPHA2 and PTPRF, three cellular proteins that function in the regulation of cell–cell contacts, appeared to be degraded by E1B-55k/E4orf3 and/or E1B-55k/E4orf6 complexes. These molecules, like integrin  $\alpha 3$  (a known substrate of E1B-55k/E4orf6), are critical regulators of cell signalling, cell adhesion and cell surface modulation, and their degradation during infection is, potentially, pertinent to adenovirus propagation. The data presented in this study illustrate the broad nature of protein down-regulation mediated by adenovirus.

## INTRODUCTION

Adenoviruses are non-enveloped, icosahedral particles containing a linear double-stranded DNA (dsDNA) genome that is approximately 36 kbp in size. Adenovirus (Ad) was originally isolated from human adenoids in tissue culture in 1953 [1] and since then has been widely studied as a model viral system and as a powerful tool for uncovering fundamental cellular processes from cell-cycle control to splicing [2–4]. As part of its wide-ranging effects in the infected cell, adenovirus triggers virally induced degradation of cellular proteins to facilitate its own replication. Through early region 1A and 1B (E1A and E1B) and E4 proteins it has been known for some time that adenovirus induces the specific degradation of host-cell proteins to favour viral replication [5, 6]. A well-understood target is the cellular DNA damage response (DDR), principally the Mre11-Rad50-Nbs1 (MRN) complex, which would normally be triggered

as the viral linear dsDNA genome builds up in the cell, mimicking extensive dsDNA breaks in the host-cell genome [7]. To counteract this, the adenoviral E1B-55k/E4orf6 proteins cooperate to redirect a cullin-containing ubiquitin ligase to specifically target a key component of the DDR known as MRE11. This consequently inhibits activation of the protein kinases ATM and ATR (reviewed in [8]). Other substrates of the E1B-55k/E4orf6 complex that are independent of MRN and play a major role in the host-cell intrinsic defence mechanism against adenovirus include p53, DNA ligase IV, integrin  $\alpha 3$ , Bloom helicase, DAXX/ATR, Tip60 and SPOC1 [9–15].

The adenovirus E4orf3 protein is also critical for inducing specific degradation of host proteins. Following infection, this viral protein reorganizes promyelocytic leukaemia (PML) nuclear bodies into distinctive track-like structures in the nucleus, where it then transiently binds to E1B-55k

Received 4 January 2017; Accepted 18 March 2017

**Author affiliations:** <sup>1</sup>School of Cellular and Molecular Medicine, University Walk, University of Bristol, Bristol BS8 1TD, UK; <sup>2</sup>Institute of Cancer and Genomic Sciences, College of Medical and Dental Sciences, University of Birmingham, Edgbaston, Birmingham B15 2TT, UK; <sup>3</sup>Proteomics Facility, Faculty of Biomedical Sciences, University Walk, University of Bristol, Bristol BS8 1TD, UK.

**\*Correspondence:** David A. Matthews, d.a.matthews@bristol.ac.uk

**Keywords:** adenovirus; d11520; E1B-55k; proteomics.

**Abbreviations:** Ad, adenovirus; DDR, DNA damage response; E1A, early region 1A; E1B, early region 1B; MRN, Mre11-Rad50-Nbs1 complex; MS/MS, tandem mass spectrometry; TMT, tandem mass tagging.

Two supplementary tables are available with the online Supplementary Material.

[16, 17]. It is thought that E4orf3 sequesters MRN components into these tracks and forms a complex with E1B-55k and E4orf6 in order to transport MRN to cytoplasmic aggregates for the degradation of MRE11 [18, 19]. Even in the absence of E1B-55K and E4orf6, the relocalization of MRN to nuclear tracks by E4orf3 alone is enough to inactivate the DDR [20]. In fact, it has been shown that E4orf3 can independently utilize the ubiquitin–proteasome pathway to promote the degradation of transcriptional intermediary factor 1 $\gamma$  (TIF1 $\gamma$ ) [21]. An additional cellular substrate of E4orf3 has recently been identified; the general transcription factor II-I (GTF2I) is targeted by E4orf3 for ubiquitination and proteasomal degradation, which stimulates gene expression from a GTF2I-repressed viral promoter [22].

Allied to these observations, genetically modified adenoviruses that are deleted for one or more viral early gene(s) have been developed for experimental and clinical purposes (reviewed in [23, 24]). An adenovirus deletion mutant called dl1520 (also known as ONYX-015) that lacks the *E1B-55k* gene product is the first conditionally replicating adenovirus tested in humans to treat cancer [25]. This mutant virus was reported in 1987 [26] and from 1996 was developed as an anti-cancer agent in clinical trials in the United States [27]. The dl1520 virus was originally thought to selectively replicate in and lyse p53-deficient cancer cells. However, increasing evidence revealed that the precise role of p53 in determining dl1520 replication selectivity was unclear [28–31]. Current evidence suggests that both p53 inactivation and preferential viral late RNA export, which has been proposed to determine the tumour selectivity of the E1B-55k-deleted oncolytic adenovirus, are associated with E1B-55k-mediated ubiquitination [9, 32, 33]. A system-wide comparison of protein abundance in wild-type adenovirus- and dl1520-infected human cells should provide greater information on how E1B-55k affects the host cell.

Quantitative tandem mass spectrometry (MS/MS)-based proteomics is widely used to identify and quantify a large number of proteins in a high-throughput manner. Tandem mass tagging (TMT) of peptide samples enables multiplex relative quantitation by mass spectrometry (MS). This approach has been utilized to identify a large number of proteins and quantitate the relative abundance of proteins in response to stimuli [34, 35]. In this study, we used this technique to identify proteins that are depleted in wild-type adenovirus-infected cells and/or dl1520-infected cells.

We have previously published a dataset of quantitative proteomics to identify proteins that may be subjected to degradation by wild-type adenovirus [36]. This study represents a more focused analysis of the role of E1B-55k in virally mediated degradation of cellular proteins, as this protein and its effects on cellular protein degradation have been widely studied. We analysed protein abundance changes in A549 cells during wild-type or dl1520 virus infection using time-course proteomics. This study provides the first global analysis of E1B-55k-associated protein expression changes in human carcinoma cells. Moreover, we validated E1B-

55k-mediated degradation of more novel proteins in adenovirus-infected cells, and identified those early-region adenovirus proteins that contribute to their degradation. Thus, we showed that quantitative proteomic analysis of virally infected cells is effective at identifying novel targets of specific virally induced degradation. Moreover, the dataset provides insights into the abundance changes of almost 5900 cellular proteins that occur during wild-type adenovirus or dl1520 infection. This should serve as a useful resource, potentially leading to a greater understanding of the role of E1B-55k during infection.

## RESULTS

### Comparative proteome analysis of wild-type, and E1B-55k-deletion, adenovirus-infected cells

To gain a comprehensive overview of the whole-cell protein expression in response to infection by wild-type human adenovirus type 5 (Ad5) or E1B-55k-deleted adenovirus (dl1520), we exploited 10-plex TMT quantitation to compare relative protein abundance over a time course. As A549 cells are highly permissive for both Ad5 and dl1520 adenovirus infection [29], we used A549 cells as the host cells in this study. We first examined the accumulation of viral early and viral late proteins in A549 cells, as a function of time of infection. The results of the preliminary experiments were used to design a time series that covered the virus infectious cycle, while focusing on the period (6–24 h after infection) in which the synthesis of viral macromolecules and changes in viral protein expression were maximal. Western blot analysis showed that the viral-early E2A DBP and E1B-55k proteins were expressed at 12 h post-infection (h p.i.) (Fig. 1a, b), while the viral-late protein VI (pVI) was produced at 18 h p.i. (Fig. 1b).

At four time points following Ad5 or dl1520 infection (6, 12, 18 and 24 h) with uninfected cells (0 h), Ad5- and dl1520-virus-infected A549 cells were harvested, and cells from the nine experiments were processed as described in the Methods section for quantitative proteomic analyses. The raw data files were processed and quantified using Proteome Discoverer software. At a false discovery rate (FDR) of 1%, this analysis identified 8190 proteins (Table S1, available in the online Supplementary Material). For further proteome analysis, the protein abundance ratio was represented for wild-type or dl1520 adenovirus-infected cells compared to uninfected cells. We retained proteins identified and quantitated by at least two peptides and with an abundance ratio variability of less than 200%. Protein abundance ratios are normally reported as the median value of all the ratios from peptides quantitated and identified as belonging to the protein in question. Allied to this, the abundance ratio variability percentage is an indicator of how divergent the peptide ratios used to calculate a particular protein ratio are – large percentage values indicate that individual peptides may be reporting very different abundance ratios, which in our experience means that the median value may be misleading (Table S1). Any protein exhibiting a 2.5-fold-or-

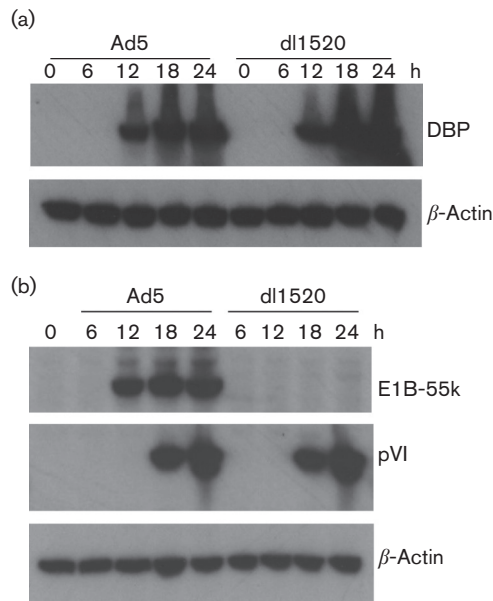


**Fig. 1.** Infection of A549 cells with Ad5 and dl1520. A549 cells were infected with Ad5 and dl1520 at a multiplicity of infection (MOI) of 10 for 0, 6, 12, 18 and 24 h. The cell lysates were harvested and the presence of the viral proteins DBP (a), E1B-55k (b) and pVI (b) were monitored as markers of viral infection by Western blotting.  $\beta$ -Actin was an internal control.

greater increase, or a 50% decrease, based on the protein relative abundance of proteins at 24 h p.i., was flagged as having significantly changed abundance. By this criterion, following virus infection, more than 5300 proteins were apparently unchanged in protein abundance, and less than 5% of identified proteins were changed in abundance (Fig. 2a). The number of virus down-regulated proteins gradually increased during virus infection (Fig. 2b). The quality of the proteome-wide quantitation was demonstrated by the consistency of the dynamic MS-based profiles for key marker proteins (Fig. 2c, d). In line with previous studies, MRE11 and p53, two known targets of E1B-55k/E4orf6 E3 ubiquitin ligase, were decreased during wild-type adenovirus infection, whilst in dl1520-infected A549 cells, MRE11 protein levels remained unchanged and p53 protein abundance increased significantly (Fig. 2c). Moreover, in agreement with observations reported by research groups [37, 38], a transient increase in p53 protein abundance early in Ad5 infection (at 6 h p.i.) and during dl1520 infection (6–24 h p.i.) was also determined in the MS analysis (Fig. 2c).

### Adenovirus E1B-55k protein regulates expression of cellular proteins and cellular programmes

To understand the cellular programmes regulated by the altered proteins during Ad5 infection and dl1520 infection, we performed biological pathway enrichment analysis using the Reactome database [39, 40]. This revealed that the changes induced spanned a broad range of categories (Fig. 3

and Table S2). During wide-type adenovirus (Ad5) infection, the cellular proteins most affected were associated with chromatin organization, DNA replication and cell cycle at 6 h p.i.; with chromatin organization, DNA replication and cellular responses to stress at 12 h p.i.; with DNA replication, cellular responses to stress and DNA repair at 18 h p.i.; and with DNA replication, cellular responses to stress and cell cycle at 24 h p.i. (Table S2). Compared to Ad5 infection, during dl1520 infection there were fewer cellular proteins affected in the early phase (Fig. 3a, b), whereas during the late phase the number of cellular proteins affected was comparable to the changes seen during Ad5 infection (Fig. 3c, d) and the cellular proteins most affected were implicated in DNA replication and cellular responses to stress and cell cycle (Table S2). The expression of the viral early E2A DBP and E1B-55k proteins and the late protein VI (pVI) shown in Fig. 1, illustrates that the two viruses were at comparable stages in their viral replication cycles in this experiment.

### Protein abundance is not exclusively regulated by E1B-55k

We first identified those proteins that decreased significantly during Ad5 infection: 69 proteins were shown to be decreased more than twofold in response to Ad5 infection. Secondly, the 69 proteins degraded during Ad5 infection were examined to see how their abundance changed during dl1520 infection to highlight those proteins whose degradation may be at least partly E1B-55k mediated. The results are shown in Table 1. Among the 69 proteins, 41 exhibited a 50% decrease in dl1520-infected A549 cells. Thus, many cellular proteins may be degraded by adenovirus by mechanisms independent of E1B-55k status. This is consistent with a recent study showing that GTF2I degradation is dependent upon adenovirus E4orf3 expression [22], something also reflected in this data set. We have also included RNA-Seq data on changes to gene expression during adenovirus infection, which we reported in an earlier study of adenovirus infection of HeLa cells [36]. However, changes in gene expression as a proxy for protein expression need to be treated cautiously, as this does not take into account other factors that affect protein abundance, such as translation initiation, whether a protein is exported from the cell, or the half-life of proteins.

### The adenovirus early-region proteins E1B-55k, E4orf3 and E4orf6 mediate the removal of the cellular proteins ALCAM, EPHA2 and PTPRF

Comparing protein abundance changes between Ad5-infected A549 cells and dl1520-infected A549 cells, our data highlighted cellular proteins previously known to be targeted by adenovirus for E1B-55k-mediated degradation, including MRE11, RAD50 and NBN (also known as NBS1) [7] (Table 2). We looked for additional cellular targets with a similar pattern of degradation during Ad5 infection: that is, a decline in protein abundance in the presence of E1B-55k. More than ten proteins meeting this criterion were identified, including three cell-adhesion molecules, ALCAM (CD166), EPHA2 (Eck) and PTPRF (LAR). As cell-adhesion

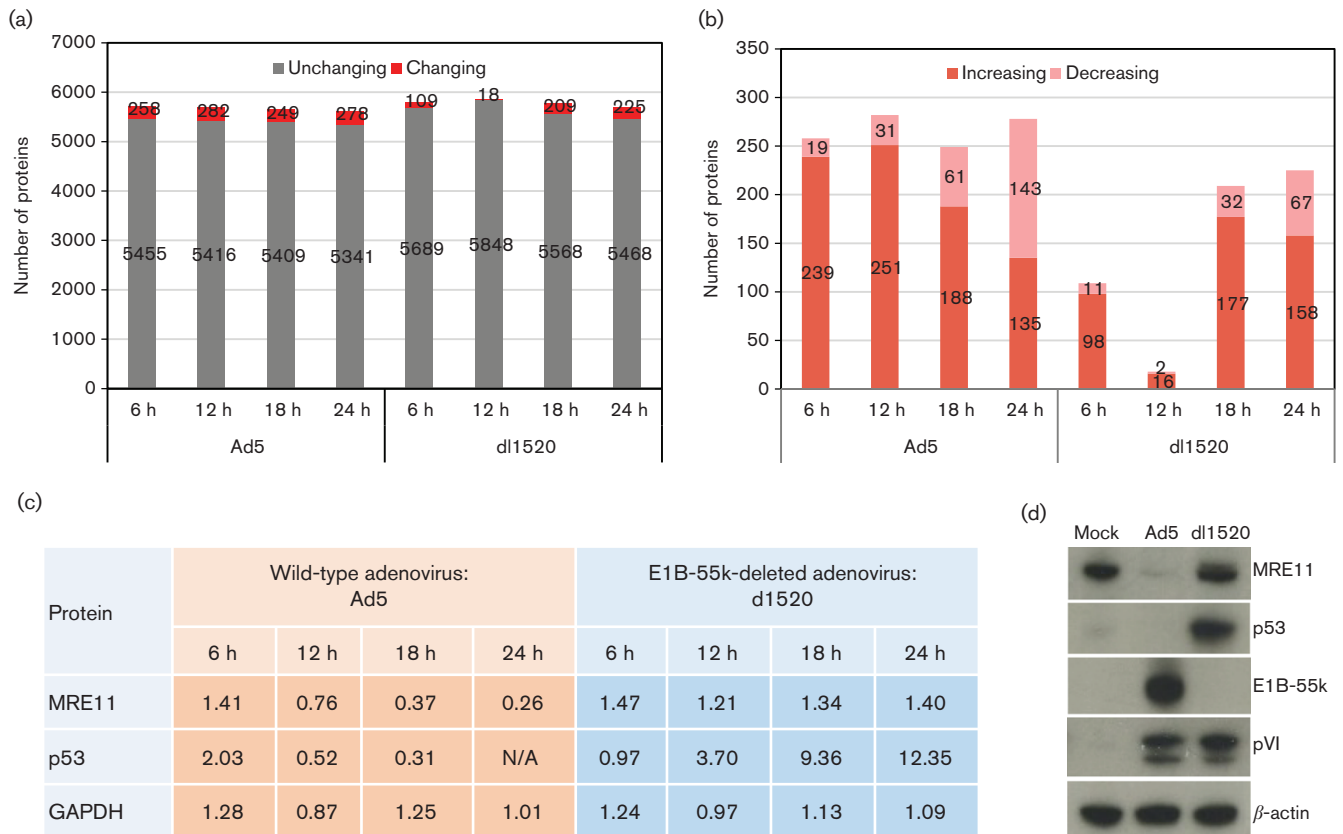


**Fig. 2.** TMT-based proteomic time course of protein expression in adenovirus-infected A549 cells. Ad5- and dl1520-virus-infected A549 cells were sampled over 24 h and the relative abundance of cellular proteins was monitored by an LC-MS/MS system. We used proteins identified by at least two peptides in this analysis. (a) Summary of the proteomics data. The number of proteins exhibiting a change in abundance (changing) or remaining unchanged (unchanging) after Ad5 or dl1520 infection of A549 cells at all time points is indicated. (b) The number of proteins that showed a 2.5-fold-or-greater increase (increasing) or a 50% decrease (decreasing) during infection. (c) Temporal profiles of MRE11 and p53 obtained in the MS/MS analysis. GAPDH was an internal control. The protein abundance ratio is shown for wild-type or dl1520 adenovirus-infected cells compared to uninfected cells. N/A indicates no abundance ratio could be determined in that experiment, even though the protein was identified. (d) The cell lysates harvested at 24 h p.i. were assessed for the presence of the cellular proteins MRE11 and p53 by Western blotting. The viral early protein E1B-55k and viral late protein pVI were monitored as markers of adenoviral infection.  $\beta$ -Actin served as a loading control.

molecules play roles in cell detachment and promoting the release and spread of progeny virions, they may represent important new substrates for degradation by the E1B-55k/E4orf6 E3 ubiquitin ligase, and therefore we decided to analyse this class of cell proteins further (Table 2).

In order to independently validate the TMT data for the selected proteins, we performed Western blot analysis on Ad5-infected A549 cells treated with the proteasome inhibitor, MG132. The results confirmed that the protein levels of ALCAM, EPHA2 and PTPRF declined significantly in A549 cells infected with Ad5 virus (Fig. 4a). However, only the degradation of EPHA2 and ALCAM was sensitive to proteasome inhibition by MG132. When cells were treated with 20  $\mu$ M MG132, EPHA2 and ALCAM the protein levels in Ad5-infected cells remained comparable to those of mock-infected cells, whereas, surprisingly, PTPRF levels were decreased in MG132-treated cells, even without viral

infection. These results suggested that proteasome activity is required for adenovirus-mediated EPHA2 and ALCAM reduction. Since MG132 alone triggers degradation of PTPRF protein, its virally triggered degradation pathway remains less clear.

We next examined which early region proteins, E1B-55k, E4orf3 and/or E4orf6, were involved in the adenovirus-induced degradation of these target proteins, or whether an alternative degradative pathway had occurred. We examined the effect of wild-type or early-region gene-mutated adenovirus [E1B-55k-(dl1520), E4orf3-(pm4150), E4orf6-(pm4154), E4orf3-/E4orf6-(pm4155)] infection on ALCAM, EPHA2 and PTPRF (Fig. 4b). Allied to this, we wanted to determine if these adenovirus proteins alone could affect levels of these cellular proteins by transfecting A549 cells with plasmids expressing one or two viral early proteins (Fig. 4c). Intriguingly, although wild-type adenovirus (wt) reliably

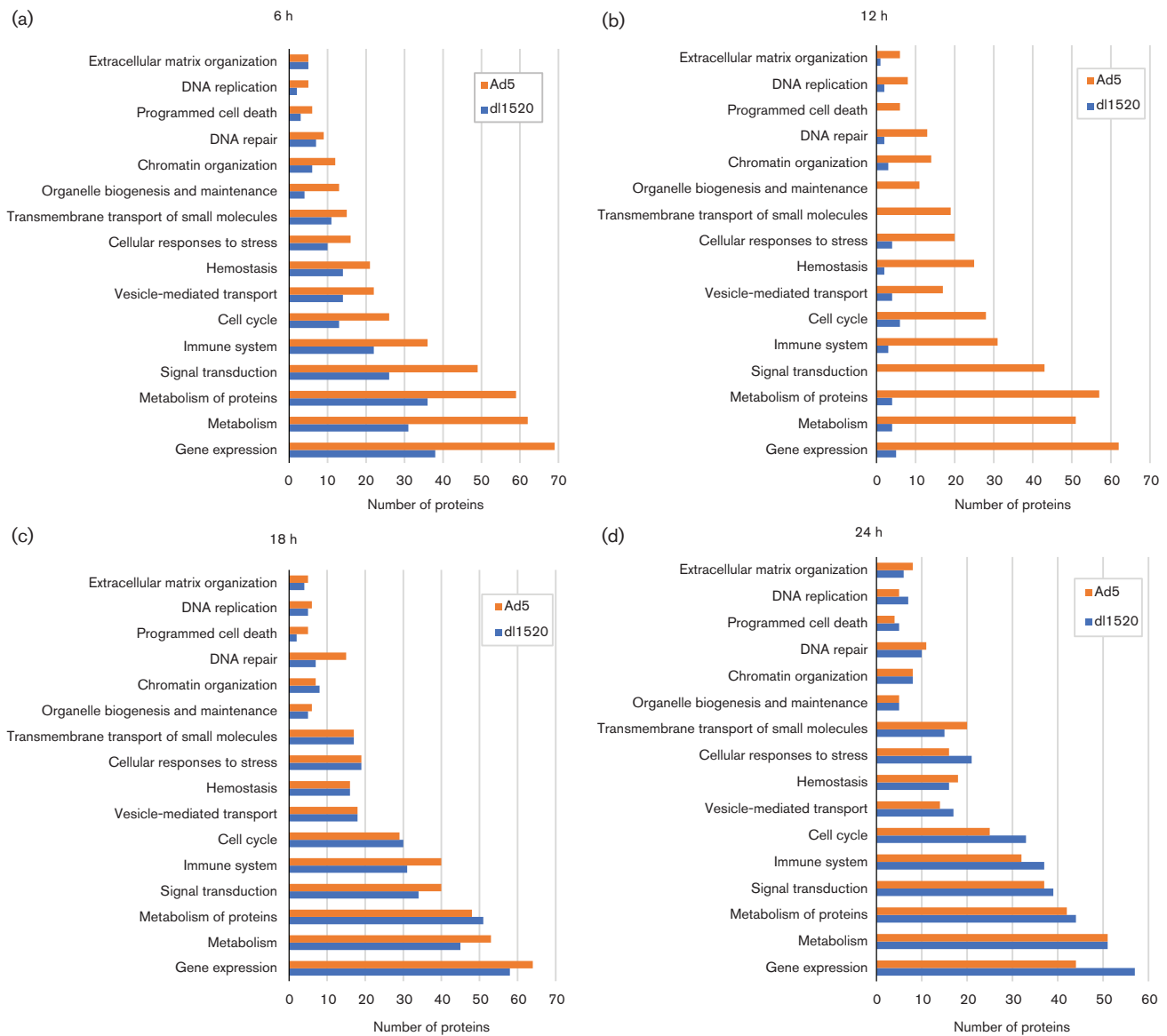


**Fig. 3.** Biological pathway enrichment analysis using the Reactome database. Cellular proteins exhibiting changes during Ad5 infection and during dl1520 were analysed by the Reactome database ([www.reactome.org/](http://www.reactome.org/)): (a) 6 h post-infection; (b) 12 h post-infection; (c) 18 h post-infection; (d) 24 h post-infection. The number of proteins is indicated at the bottom of the figure. Ad5-regulated proteins are shown in orange and dl1520-regulated proteins are shown in blue.

degraded ALCAM, PTPRF and EPHA2, the pathways triggering their degradation appear to be distinct and complex. From the transfection studies, expression of E4orf6 alone, or E1B-55k/E4orf3 or E1B-55k/E4orf6 combinations, can target ALCAM for some degradation (Fig. 4c). A549 cells infected with a virus lacking either E1B-55k or E4orf3 showed partial degradation of ALCAM, but the protein levels of ALCAM in cells infected with a virus lacking E4orf6 or E4orf3 and E4orf6 together remained unchanged (Fig. 4b). These results implicate E4orf6, E1B-55k/E4orf6 and E4orf3/E4orf6 in degradation of ALCAM. PTPRF levels decreased in A549 cells infected with a viral mutant that does not express E4orf3

(pm4150) or E4orf6 (pm4154), but were unaffected by E1B-55k-deleted (dl1520) and E4orf3/E4orf6-deleted viruses (pm4155) (Fig. 4b). The reduction of PTPRF was detected in A549 cells expressing either E1B-55k/E4orf3 or E1B-55k-E4orf6 (Fig. 4c) and partial degradation was observed by those expressing E4orf6 alone (Fig. 4c). The reduction in EPHA2 was still evident following infection with either E4orf3-deleted virus or E4orf6-deleted virus (Fig. 4b), while from transfection studies, E1B-55k/E4orf6 was involved in the reduction of EPHA2 (Fig. 4c). We determined that proteasome activity is required for ALCAM and EPHA2 reduction (Fig. 4a), and the effects of adenovirus infection on

**Table 1.** Proteins decreased in A549 cells infected with adenovirus

A list of proteins that decreased in abundance more than twofold in Ad5- and/or dl1520-infected A549 cells compared to uninfected A549 cells at 24 h p.i.; the data were generated in this study. Fold change in gene expression between Ad5-infected HeLa cells at 24 h p.i. and uninfected HeLa cells; the RNA-Seq data were obtained from our previous studies [36].

| UniProt accession   | Protein description  | Gene name | mRNA fold change in HeLa cells |
|---|--|-----------|--------------------------------|
| <b>Protein decreased in amount &gt;twofold during Ad5 infection and during dl1520 infection</b>                             |  |           |                                |
| A0A024RCT1  | TAP binding protein (Tapasin), isoform CRA_c               | TAPBP     | 0.56                           |
| P55268  | Laminin subunit beta-2                                     | LAMB2     | 1.56                           |
| X5CMH5  | TAP2   | TAP2      | 3.92                           |
| Q99650  | Oncostatin-M-specific receptor subunit beta                | OSMR      | 1.03                           |
| B2RMV2  | CYTSA protein  | CYTSA     | 2.15                           |
| P35568  | Insulin receptor substrate 1                               | IRS1      | 0.24                           |
| Q0IIN7  | Nuclear receptor coactivator 3                             | NCOA3     | 0.79                           |
| P05121  | Plasminogen activator inhibitor 1                          | SERPINE1  | 0.11                           |
| Q8N6N3  | UPF0690 protein C1orf52                                    | C1orf52   | 0.46                           |
| Q14641  | Early placenta insulin-like peptide                        | INSL4     | 0                              |
| B7Z168  | Neuregulin 1 isoform HRG-alpha                             | NRG1      | 0                              |
| Q9UK54  | Haemoglobin beta subunit variant                           | HBB       | Not detected                   |
| X5D2J9  | General transcription factor Ili isoform D                 | GTF2I     | 0.79                           |
| Q7Z5L9  | Interferon regulatory factor 2-binding protein 2           | IRF2BP2   | 0.61                           |
| P15428  | 15-hydroxyprostaglandin dehydrogenase [NAD(+)]             | HPGD      | 0.72                           |
| P17676  | CCAAT/enhancer-binding protein beta                        | CEBPB     | 0.24                           |
| H0Y485  | Insulin-like growth factor-binding protein 3               | IGFBP3    | 0.87                           |
| P40189  | Interleukin-6 receptor subunit beta                        | IL6ST     | 0.97                           |
| A0A087WV90  | Dystrophin   | DMD       | 1.19                           |
| Q12860  | Contactin-1  | CNTN1     | Not detected                   |
| Q8IY57  | YY1-associated factor 2                                    | YAF2      | 0.6                            |
| Q9NPA3  | Mid1-interacting protein 1                                 | MID1IP1   | 0.35                           |
| Q5MJ32  | Protection of telomeres protein 1 variant 5                | POT1      | 1.36                           |
| O00767  | Acyl-CoA desaturase  | SCD       | 2.64                           |
| A2AJT9  | Uncharacterized protein CXorf23                            | CXorf23   | 0                              |
| Q8IUC4  | Rhophilin-2  | RHPN2     | 0.55                           |
| Q5VUA4  | Zinc finger protein 318                                    | ZNF318    | 0.41                           |
| O14757  | Serine/threonine-protein kinase Chk1                       | CHEK1     | 1.16                           |
| P14384  | Carboxypeptidase M   | CPM       | 1.28                           |
| O43318  | Mitogen-activated protein kinase kinase kinase 7           | MAP3K7    | 0.7                            |
| P35869  | Aryl hydrocarbon receptor                                  | AHR       | 0.29                           |
| Q8NCD3  | Holliday junction recognition protein                      | HJURP     | 0.11                           |
| P78545  | ETS-related transcription factor Elf-3                     | ELF3      | 0.07                           |
| Q07973  | 1,25-dihydroxyvitamin D(3) 24-hydroxylase, mitochondrial   | CYP24A1   | 0.18                           |
| A0A087WWW9  | B-cell lymphoma/leukaemia 10                               | BCL10     | 0.31                           |
| P35354  | Prostaglandin G/H synthase 2                               | PTGS2     | 0                              |
| Q59GZ8  | Urokinase plasminogen activator preproprotein variant      | PLAUR     | 0.79                           |
| P63313  | Thymosin beta-10   | TMSB10    | 0.54                           |
| B2RUU3  | Dedicator of cytokinesis 1                                 | DOCK1     | 0.28                           |
| F5H7B7  | ATP-binding cassette sub-family A member 13                | ABCA13    | Not detected                   |
| P62328  | Thymosin beta-4  | TMSB4X    | Not detected                   |
| <b>Protein decreased in amount twofold during Ad5 infection and slightly decreased (1.5–2 fold) during dl1520 infection</b> |  |           |                                |
| H3BS02  | [3-methyl-2-oxobutanoate dehydrogenase (lipoamide)] kinase | BCKDK     | 1.3                            |
| Q6QWC0  | TAP1   | TAP1      | Not detected                   |
| Q9NZV1  | Cysteine-rich motor neuron 1 protein                       | CRIM1     | 0.24                           |
| Q13641  | Trophoblast glycoprotein                                   | TPBG      | 0.48                           |
| Q96L35  | EPH receptor B4, isoform CRA_b                             | EPHB4     | 0.51                           |
| Q96HR8  | H/ACA ribonucleoprotein complex non-core subunit NAF1      | NAF1      | 1.19                           |

Table 1. cont.

| UniProt accession  | Protein description   | Gene name | mRNA fold change in HeLa cells |
|--|---|-----------|--------------------------------|
| P17275   | Transcription factor jun-B  | JUNB      | 0.17                           |
| A2ACR1   | Proteasome subunit beta type                                      | PSMB9     | Not detected                   |
| Q9H1E3   | Nuclear ubiquitous casein and cyclin-dependent kinase substrate 1 | NUCKS1    | 1                              |
| Q96DI9   | POLDIP3 protein   | POLDIP3   | 0.87                           |
| Q96BU1   | S100P-binding protein   | S100PBP   | 1.36                           |
| H3BUT5   | Nuclear envelope phosphatase-regulatory subunit 1                 | CNEP1R1   | 0                              |
| A0A024R4D3   | Melanophilin, isoform CRA_b                                       | MLPH      | Not detected                   |
| Q9UMY1   | Nucleolar protein 7   | NOL7      | 1.11                           |
| Q6IE81   | Protein Jade-1  | JADE1     | 0.37                           |
| Q6MZZ4   | Putative uncharacterized protein DKFZp686H0575                    | ELF1      | 0.45                           |
| Q14814   | Myocyte-specific enhancer factor 2D                               | MEF2D     | 0.56                           |
| <b>Protein decreased in amount &gt;twofold during Ad5 infection but did not decrease during dl1520 infection</b> |   |           |                                |
| B6E4×6   | Cellular tumour antigen p53                                       | p53       | 1.24                           |
| P49959   | Double-strand break repair protein MRE11A                         | MRE11A    | 2.16                           |
| Q92878   | DNA repair protein RAD50  | RAD50     | 2.18                           |
| Q13740   | CD166 antigen   | ALCAM     | 1.36                           |
| P29317   | Ephrin type-A receptor 2  | EPHA2     | 0.41                           |
| F1T0K4   | DmX-like protein 1  | DMXL1     | 0.89                           |
| E9PMH5   | Baculoviral IAP repeat-containing protein 2                       | BIRC2     | 0.49                           |
| O60934   | Nibrin  | NBN       | 1.19                           |
| Q8NAF0   | Zinc finger protein 579   | ZNF579    | 0                              |
| P10586   | Receptor-type tyrosine-protein phosphatase F                      | PTPRF     | 4.71                           |
| Q7Z589   | Protein EMSY  | EMSY      | 0.69                           |

ALCAM and EPHA2 levels (Fig. 4b, c) support the contention that at least the E1B-55k/E4orf6 complex targets ALCAM and EPHA2 for ubiquitination and subsequent proteasome-mediated degradation.

## DISCUSSION

In this time-course study, global analysis of the host proteome remodelling during adenovirus infection was performed using a more focused approach: comparing protein abundance in wild-type vs E1B-55k-deletion-mutant adenovirus-infected cells. This produced a temporal map of protein abundance changes for 5937 proteins in Ad5-infected A549 cells

compared to dl1520-infected A549 cells. Bioinformatics analysis using the Reactome database revealed that the adenovirus-regulated proteins were involved in several cellular programmes, including chromatin organization, DNA replication, cell cycle and cellular response to stress (Fig. 3 and Table S2).

Adenovirus early-region proteins interact together to modify critical cellular pathways and prepare the host cell for viral replication. As a key example of this, E1B-55k, E4orf3 and E4orf6 have been the subject of much research and there are several well-characterized interactions between these viral proteins and the host cells (reviewed in [41]). Our proteomics data revealed some 69 cellular proteins that are degraded

Table 2. Proteins decreased in A549 cells infected with Ad5, but remained unchanged during dl1520 infection

| Protein name | Ad5* |      |      |      | dl1520† |      |      |      |
|--------------|------|------|------|------|---------|------|------|------|
|              | 6 h  | 12 h | 18 h | 24 h | 6 h     | 12 h | 18 h | 24 h |
| MRE11A‡      | 1.41 | 0.76 | 0.37 | 0.26 | 1.47    | 1.21 | 1.34 | 1.40 |
| RAD50‡       | 1.35 | 0.69 | 0.35 | 0.30 | 1.38    | 1.28 | 1.29 | 1.21 |
| NBN‡         | 1.18 | 1.19 | 0.58 | 0.42 | 1.23    | 1.21 | 1.10 | 0.92 |
| ALCAM        | 1.11 | 0.77 | 0.52 | 0.47 | 1.07    | 1.20 | 1.37 | 1.14 |
| EPHA2        | 1.24 | 1.23 | 0.54 | 0.46 | 1.32    | 1.24 | 1.23 | 1.09 |
| PTPRF        | 0.79 | 0.85 | 0.59 | 0.43 | 0.82    | 0.81 | 0.74 | 0.73 |

\*Protein abundance ratio is shown for wild-type adenovirus (Ad5)-infected cells compared to mock-infected cells.

†Protein abundance ratio is shown for E1B-55k-deleted adenovirus (dl1520)-infected cells compared to mock-infected cells.

‡Known cellular proteins whose levels are reduced via adenoviral E1B-55k functions.



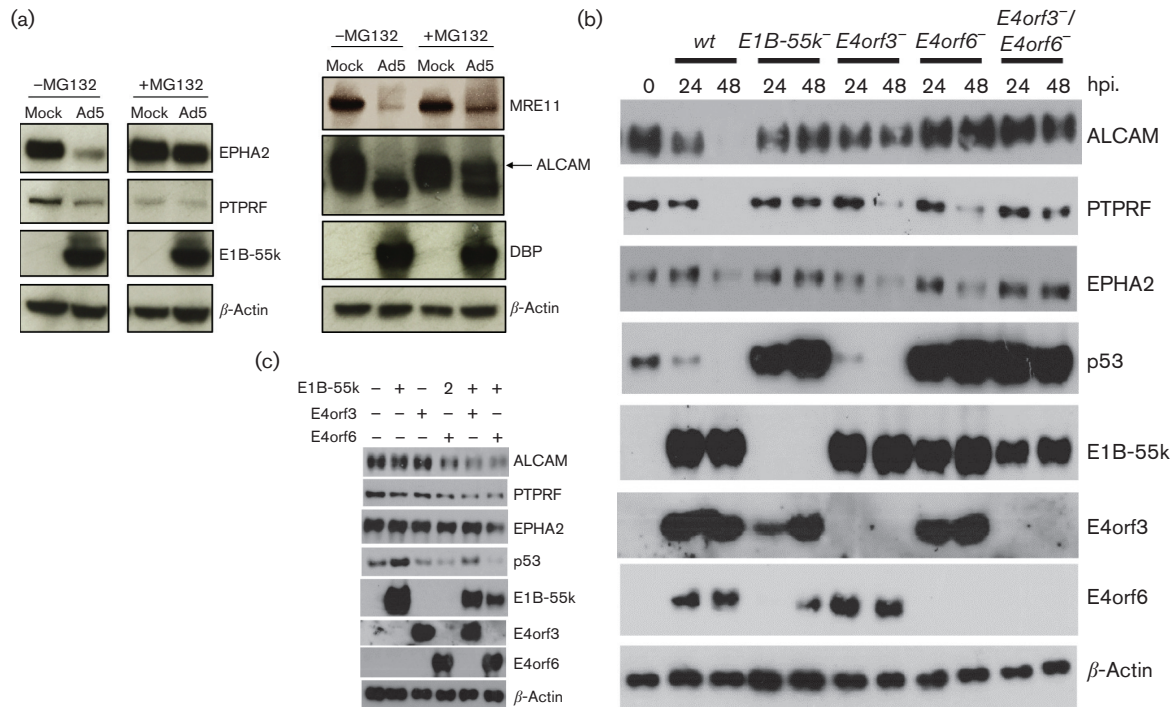


**Fig. 4.** Ad5-induced degradation of the cellular proteins ALCAM, EPHA2 and PTPRF is mediated by the adenovirus early-region proteins E1B-55k, E4orf3 and/or E4orf6. (a) Effect of proteasome inhibition on ALCAM, EPHA2 and PTPRF levels. A549 cells were uninfected (mock) or infected with Ad5 or dl1520 at an MOI of 10. After 6 h the uninfected and adenovirus-infected cells were treated with the proteasome inhibitor MG132 at a final concentration of 20  $\mu$ M. The cells were incubated under normal conditions for a further 18 h and then harvested. ALCAM, EPHA2, PTPRF, MRE11, E1B-55k and DBP were visualized by immunoblotting using the appropriate antibodies.  $\beta$ -Actin served as a loading control. The left-hand part of the panel was cropped from the same gel exposure in the case of each of the antigens shown. (b) Infection of A549 cells. A549 cells were left uninfected or infected with either Ad5 or mutant Ad5 preparations at an MOI of 5. Total cell extracts were prepared 24 and 48 h p.i., and proteins were separated by SDS-PAGE and subjected to immunoblotting using E1B-55k, E4orf3, E4orf6, p53, ALCAM, EPHA2 and PTPRF antibodies.  $\beta$ -Actin served as a loading control. (c) A549 cells were transfected with plasmids expressing combinations of adenovirus E1B-55k, E4orf3 and E4orf6, as indicated. After 48 h the total cell lysate was harvested and, as before, cellular proteins were detected by Western blots with  $\beta$ -actin used as a loading control.

following adenovirus infection, but of these, E1B-55k appears to be required for the shut-off and removal of just 11 cellular proteins, some novel and some previously known (Table 1).

Dallaire *et al.* [10] identified the cell-surface molecule, integrin  $\alpha$ 3, as a substrate of the E1B-55k-mediated E3 ligase complex and suggested that other adhesion molecules may also be affected by E4orf6/E1B-55k. In this study, we found that three novel cell adhesion molecules, ALCAM, EPHA2 and PTPRF, are affected by E1B-55k, E4orf6 and/or E4orf3, and the pathways triggering their degradation are more complex than has previously been reported.

ALCAM protein was degraded by wild-type adenovirus (Fig. 4b) and the analysis of infection with single or double mutants revealed that there appear to be two or more mechanisms promoting degradation. In the context of transfection experiments (Fig. 4c), the degradation of ALCAM appears to occur on the expression of E4orf6 alone, E1B-55k/E4orf3 or E1B-55k/E4orf6. In the context of a full

virus infection, E4orf6 is required for ALCAM reduction (Fig. 4b). In addition, removal of ALCAM is dependent on the proteasome activity (Fig. 4a). Together, these data suggest that ALCAM is a target of adenoviral E1B-55k/E4orf6 ubiquitin ligase. However, additional studies will be required to explain in detail how adenovirus infection modulates overall ALCAM abundance.

Nevertheless, degradation of ALCAM may be a strategy for cell detachment and restricting immune surveillance via adenovirus-induced targeted ubiquitination. ALCAM, also known as CD166, is an activated leukocyte cell-adhesion molecule that mediates both heterotypic cell–cell contacts and homotypic cell–cell contacts [42, 43]. In addition, ALCAM has been identified as a bona fide target of viral protein K5, a modulator of immune recognition from Kaposi's sarcoma-associated herpesvirus, which prevents activation of cytotoxic T cells and natural killer cells [44]. Potentially, the clearance of ALCAM during infection might inhibit

ALCAM-dependent immune responses and promote adenovirus propagation.

EPHA2, also called Eck (epithelial cell kinase), is a receptor tyrosine kinase that binds to membrane-bound ephrin-A family ligands and functions to regulate cell migration and cell growth [45]. Our data suggest that EPHA2 is a novel substrate for Ad5 E1B-55k-mediated proteasomal degradation. Studies with mutant adenoviruses revealed that EPHA2 degradation is dependent upon E1B-55k/E4orf6 expression (Fig. 4b, c). However, our data also suggest that there might be redundant pathways involved in the E1B-55k/E4orf3-mediated EPHA2 reduction (Fig. 4b, c).

PTPRF, also known as LAR (leukocyte common antigen related), is a receptor-like protein tyrosine phosphatase located in the plasma membrane. The degradation of PTPRF appears to be dependent upon adenoviral E1B-55k/E4orf6 or E1B-55k/E4orf3 protein expression (Fig. 4b, c). However, as PTPRF protein levels were reduced in MG132-treated uninfected A549 cells via an unknown mechanism (Fig. 4a), further work is required to determine exactly how adenovirus reduces overall levels of this protein in the cell. Evidence from recent work indicates that PTPRF modulates cell migration through dephosphorylating EPHA2 [46]. The EPHA2 receptor is also known to interact with integrin  $\alpha 3$  (a known substrate of the E1B-55k/E4orf6 E3 ubiquitin ligase complex) in U251MG glioblastoma cells, and contributes to the crosstalk between Eph and integrin signalling pathways at membrane protrusions [10, 47]. Taken together, our data suggest that it is likely that adenovirus regulates cell-surface proteins through E1B-55k, and the relationship between adenovirus infection and cell-surface molecules is more complex than is currently understood.

There is also a formal possibility that the reduction of protein abundance could be an indirect result of changes in mRNA levels or it might be because adenovirus induces the export and shedding of these cellular proteins. However, as EPHA2 and ALCAM degradation is readily blocked by MG132, we argue that the weight of evidence suggests that their degradation is a post-translational effect mediated by combinations of E1B-55k and/or E4orf6 and E4orf3. For PTPRF, additional work is needed to understand exactly how adenovirus mediates this change in cellular abundance. Nevertheless, regardless of the precise mechanism, our data significantly widen the list of cell-surface proteins downregulated by adenovirus infection.

As pointed out in the Introduction, a number of proteins are known to be down-regulated by adenovirus infection (e.g. DNA ligase IV and integrin  $\alpha 3$ ), but they were not identified in this study. This reflects one of the downsides of mass-spectrometry-based proteomics, namely that it is not yet possible to guarantee that all proteins will be confidently identified and quantitated.

In conclusion, we have characterized relative protein abundance changes in A549 cells infected with wild-type adenovirus and/or E1B-55k-deleted adenovirus. From these data

we have obtained a range of novel cellular proteins targeted by adenovirus for degradation, including the identification of novel E1B-55k-dependent targets. This study identifies a wider range of cellular targets for adenovirus-mediated degradation and our follow-up analysis revealed that adenovirus-mediated protein degradation may involve multiple (and potentially partially redundant) pathways. Moreover, the time-course dataset for protein abundance changes is a valuable data resource for the study of wild-type and E1B-55k-deleted adenoviruses.

## METHODS

### Cells and viruses

Human lung carcinoma cells (A549) were cultured in Dulbecco's modified Eagle's medium with  $4.5 \text{ g l}^{-1}$  glucose and L-glutamine (DMEM, Lonza), supplemented with 10 % fetal bovine serum (FBS), streptomycin ( $100 \mu\text{g ml}^{-1}$ ) and penicillin ( $100 \text{ IU ml}^{-1}$ ) (Life Technologies). Wild-type human adenovirus type 5 (Ad5) was propagated as described previously [48] and preparations were purified twice by caesium chloride density gradient centrifugation [49]. The mutant human adenovirus preparations, deleted in E1B-55k (dl1520), E4orf3 (pm4150), E4orf6 (pm4154) and E4orf3 and E4orf6 (pm4155), have been described previously [21, 26, 50]. We thank Thomas Dobner (HPI, Hamburg) for kindly providing E4orf3 (pm4150), E4orf6 (pm4154) and E4orf3 and E4orf6 (pm4155) deletion viruses.

### Adenovirus infection, TMT labelling and high pH reversed-phase chromatography

A549 cells were seeded at a concentration of  $1 \times 10^6$  cells and left overnight to adhere. The cultures were infected with either Ad5 or dl1520 at a multiplicity of infection (MOI) of 10. The cells were incubated under normal conditions for 0, 6, 12, 18 and 24 h, and then harvested and washed twice in PBS. For each sample, the cell pellets were resuspended in five-cell-pellet volumes of lysis buffer containing 8 M urea in 50 mM triethylammonium bicarbonate (TEAB) (Thermo Scientific), pH 8, and  $\times 1$  protease inhibitor cocktail (Roche, 11836170001), followed by sonication (15  $\times$  2 on ice, at 20 % output). Then, the samples were spun at 17 000 g for 10 min at  $4^\circ\text{C}$ . The protein concentration of the cell extracts was determined using the BCA protein assay kit (Thermo Fisher Scientific).

Aliquots of  $100 \mu\text{g}$  of ten samples per experiment were digested with trypsin ( $2.5 \mu\text{g}$  trypsin per  $100 \mu\text{g}$  protein;  $37^\circ\text{C}$ , overnight) and labelled with tandem mass tag (TMT) ten-plex reagents according to the manufacturer's protocol (Thermo Fisher Scientific); the labelled samples were then pooled.

A  $50 \mu\text{g}$  aliquot of the pooled sample was evaporated to dryness and resuspended in buffer A (20 mM ammonium hydroxide, pH 10) prior to fractionation by high-pH reversed-phase chromatography using an Ultimate 3000 liquid chromatography system (Thermo Fisher Scientific).

In brief, the sample was loaded onto an XBridge BEH C18 column (130 Å, 3.5 µm, 2.1 × 150 mm; Waters, UK) in buffer A and the peptides were eluted with an increasing gradient of buffer B (20 mM ammonium hydroxide in acetonitrile, pH 10) from 0–95 % over 60 min. The resulting fractions were evaporated to dryness and resuspended in 1 % formic acid prior to analysis by nano-LC MS/MS using an Orbitrap Fusion Tribrid mass spectrometer (Thermo Scientific).

### Nano-LC mass spectrometry

High-pH RP fractions were further fractionated using an Ultimate 3000 nano HPLC system in line with an Orbitrap Fusion Tribrid mass spectrometer (Thermo Scientific). In brief, peptides in 1 % (vol/vol) formic acid were injected onto an Acclaim PepMap C18 nano-trap column (Thermo Scientific). After washing with 0.5 % (vol/vol) acetonitrile 0.1 % (vol/vol), formic acid peptides were resolved on a 250 mm × 75 µm Acclaim PepMap C18 reverse-phase analytical column (Thermo Scientific) over a 150 min organic gradient, using seven gradient segments (1–6 % solvent B over 1 min, 6–15 % B over 58 min, 15–32 % B over 58 min, 32–40 % B over 5 min, 40–90 % B over 1 min, held at 90 % B for 6 min and then reduced to 1 % B over 1 min) with a flow rate of 300 nl min<sup>-1</sup>. Solvent A was 0.1 % formic acid and solvent B was aqueous 80 % acetonitrile in 0.1 % formic acid. Peptides were ionized by nano-electrospray ionization at 2.0 kV using a stainless steel emitter with an internal diameter of 30 µm (Thermo Scientific) and a capillary temperature of 275 °C.

All spectra were acquired using an Orbitrap Fusion Tribrid mass spectrometer controlled by Xcalibur 1.9 software (Thermo Scientific) and operated in data-dependent acquisition mode using an SPS-MS3 workflow. FTMS1 spectra were collected at a resolution of 120 000, with an automatic gain control (AGC) target of 200 000 and a max injection time of 50 ms. The top *N* most intense ions were selected for MS/MS. Precursors were filtered according to charge state (to include charge states 2–7) and with monoisotopic precursor selection. Previously interrogated precursors were excluded using a dynamic window (40s+/-10 p.p.m.). The MS2 precursors were isolated with a quadrupole mass filter set to a width of 1.2 *m/z*. ITMS2 spectra were collected with an AGC target of 5000, a max injection time of 70 ms and a CID collision energy of 35 %.

For FTMS3 analysis, the Orbitrap was operated at 60 000 × resolution with an AGC target of 50 000 and a max injection time of 120 ms. Precursors were fragmented by high-energy collision dissociation (HCD) at a normalized collision energy of 55 % to ensure maximal TMT reporter ion yield. Synchronous precursor selection (SPS) was enabled to include up to five MS2 fragment ions in the FTMS3 scan.

### Data analysis

The raw data files were processed and quantified using Proteome Discoverer software v1.4 (Thermo Scientific) and searched against a combined database consisting of the UniProt human database (downloaded 8 November

2014:126 385 entries) and adenovirus protein sequences using the SEQUEST algorithm. Peptide precursor mass tolerance was set at 10 ppm and MS/MS tolerance was set at 0.6 Da. Search criteria included oxidation of methionine (+15.9949) as a variable modification and carbamidomethylation of cysteine (+57.0214) and the addition of the TMT (+229.163) to peptide N-termini and lysine as fixed modifications. Searches were performed with full tryptic digestion and a maximum of one missed cleavage was allowed. The reverse database search option was enabled and all peptide data were filtered to satisfy a false discovery rate (FDR) of 1 %.

### Infection of human A549 cells with Ad5 and mutant virus and treatment with MG132

A549 cells were seeded at a concentration of 2 × 10<sup>5</sup> cells per well in a six-well plate and left overnight to adhere. The cultures were either uninfected, or infected with either Ad5 or dl1520 preps at an MOI of 10. After 6 h the uninfected and adenovirus-infected cells were treated with the proteasome inhibitor MG132 at a final concentration of 20 µM. The cells were incubated under normal conditions for a further 18 h and then harvested and washed twice in PBS. The cells were resuspended in PBS and SDS loading buffer containing 10 mM 2-mercaptoethanol and sonicated five times to ensure complete the extraction of total cellular proteins.

### Transfection of A549 cells

A549 cells were seeded at 5 × 10<sup>5</sup> cells on 6 cm dishes. Four hours after plating, the cells were washed twice in Optimem (Life Technologies) and incubated with different combinations of pcDNA3, pcDNA3-Ad5-E1B-55k, pcDNA3-Ad5-E4orf3 and pcDNA3-Ad5-E4orf6 (see Fig. 4c legend) for 6 h, in the presence of Lipofectamine 2000 (Life Technologies), according to manufacturer's recommendations. After transfection, cells were washed once in DMEM medium and incubated for an additional 24 h in DMEM before being washed twice in PBS and harvested and processed for subsequent analysis of cellular proteins by SDS-PAGE.

### Western blotting and antibodies

Test samples were first denatured by heating at 95 °C for 10 min and then separated by electrophoresis on a Tris-glycine polyacrylamide gel. Proteins were transferred to Hybond-P PVDF membrane (GE Healthcare, UK) and probed with a specific primary antibody, followed by a horseradish peroxidase (HRP)-conjugated secondary antibody. Blots were developed with the ECL detection system (GE Healthcare, UK). The primary antibodies used were monoclonal anti-DBP [48], mouse anti-E1B-55k [51], rabbit anti-pVI [48], polyclonal goat anti-MRE11, monoclonal mouse anti-p53 (Santa Cruz), polyclonal rabbit anti-ALCAM (Sino Biotechnology), polyclonal rabbit anti-β-actin (Cell Signaling), monoclonal mouse anti-Eck/EphA2 (Merck Millipore) and monoclonal mouse anti-LAR/PTPRF (BD Biosciences). Anti-E4orf3 and anti-E4orf6 antibodies were provided by Thomas Dobner (HPI, Hamburg). The secondary

antibodies used were goat anti-rabbit IgG-HRP, goat anti-mouse IgG-HRP and donkey anti-goat IgG-HRP (Santa Cruz).

#### Funding information

We would like to thank BBSRC for funding to D. A. M. (BB/M02542X/1) and A. S. T. (BB/J014532/1).

#### Conflicts of interest

The authors declare that there are no conflicts of interest.

#### References

- Rowe WP, Huebner RJ, Gilmore LK, Parrott RH, Ward TG. Isolation of a cytopathogenic agent from human adenoids undergoing spontaneous degeneration in tissue culture. *Proc Soc Exp Biol Med* 1953;84:570–573.
- Yang XJ, Ogryzko VV, Nishikawa J, Howard BH, Nakatani Y. A p300/CBP-associated factor that competes with the adenoviral oncoprotein E1A. *Nature* 1996;382:319–324.
- Berget SM, Moore C, Sharp PA. Spliced segments at the 5' terminus of adenovirus 2 late mRNA. *Proc Natl Acad Sci USA* 1977;74:3171–3175.
- Chow LT, Gelinas RE, Broker TR, Roberts RJ. An amazing sequence arrangement at the 5' ends of adenovirus 2 messenger RNA. *Cell* 1977;12:1–8.
- Moran E. Interaction of adenoviral proteins with pRB and p53. *FASEB J* 1993;7:880–885.
- Harada JN, Shevchenko A, Shevchenko A, Pallas DC, Berk AJ. Analysis of the adenovirus E1B-55K-anchored proteome reveals its link to ubiquitination machinery. *J Virol* 2002;76:9194–9206.
- Stracker TH, Carson CT, Weitzman MD. Adenovirus oncoproteins inactivate the Mre11-Rad50-NBS1 DNA repair complex. *Nature* 2002;418:348–352.
- Turnell AS, Grand RJ. DNA viruses and the cellular DNA-damage response. *J Gen Virol* 2012;93:2076–2097.
- Querido E, Blanchette P, Yan Q, Kamura T, Morrison M et al. Degradation of p53 by adenovirus E4orf6 and E1B55K proteins occurs via a novel mechanism involving a Cullin-containing complex. *Genes Dev* 2001;15:3104–3117.
- Dallaire F, Blanchette P, Groitl P, Dobner T, Branton PE. Identification of integrin alpha3 as a new substrate of the adenovirus E4orf6/E1B 55-kilodalton E3 ubiquitin ligase complex. *J Virol* 2009;83:5329–5338.
- Baker A, Rohleder KJ, Hanakahi LA, Ketner G. Adenovirus E4 34k and E1b 55k oncoproteins target host DNA ligase IV for proteasomal degradation. *J Virol* 2007;81:7034–7040.
- Orazio NI, Naeger CM, Karlseder J, Weitzman MD. The adenovirus E1b55K/E4orf6 complex induces degradation of the Bloom helicase during infection. *J Virol* 2011;85:1887–1892.
- Gupta A, Jha S, Engel DA, Ornelles DA, Dutta A. Tip60 degradation by adenovirus relieves transcriptional repression of viral transcriptional activator E1A. *Oncogene* 2013;32:5017–5025.
- Schreiner S, Bürck C, Glass M, Groitl P, Wimmer P et al. Control of human adenovirus type 5 gene expression by cellular Daxx/ATRX chromatin-associated complexes. *Nucleic Acids Res* 2013;41:3532–3550.
- Schreiner S, Kinkley S, Bürck C, Mund A, Wimmer P et al. SPOC1-mediated antiviral host cell response is antagonized early in human adenovirus type 5 infection. *PLoS Pathog* 2013;9:e1003775.
- Carvalho T, Seeler JS, Ohman K, Jordan P, Pettersson U et al. Targeting of adenovirus E1A and E4-ORF3 proteins to nuclear matrix-associated PML bodies. *J Cell Biol* 1995;131:45–56.
- Doucas V, Ishov AM, Romo A, Juguilon H, Weitzman MD et al. Adenovirus replication is coupled with the dynamic properties of the PML nuclear structure. *Genes Dev* 1996;10:196–207.
- Evans JD, Hearing P. Distinct roles of the adenovirus E4 ORF3 protein in viral DNA replication and inhibition of genome concatination. *J Virol* 2003;77:5295–5304.
- Liu Y, Shevchenko A, Shevchenko A, Berk AJ. Adenovirus exploits the cellular aggresome response to accelerate inactivation of the MRN complex. *J Virol* 2005;79:14004–14016.
- Stracker TH, Lee DV, Carson CT, Araujo FD, Ornelles DA et al. Serotype-specific reorganization of the Mre11 complex by adenoviral E4orf3 proteins. *J Virol* 2005;79:6664–6673.
- Forrester NA, Patel RN, Speiseder T, Groitl P, Sedgwick GG et al. Adenovirus E4orf3 targets transcriptional intermediary factor 1γ for proteasome-dependent degradation during infection. *J Virol* 2012;86:3167–3179.
- Bridges RG, Sohn SY, Wright J, Leppard KN, Hearing P. The adenovirus E4-ORF3 protein stimulates SUMOylation of general transcription factor TFII-I to direct proteasomal degradation. *MBio* 2016;7:e02184-15.
- Toth K, Wold WS. Increasing the efficacy of oncolytic adenovirus vectors. *Viruses* 2010;2:1844–1866.
- Russell SJ, Peng KW, Bell JC. Oncolytic virotherapy. *Nat Biotechnol* 2012;30:658–670.
- Kirn D. Clinical research results with dl1520 (Onyx-015), a replication-selective adenovirus for the treatment of cancer: what have we learned? *Gene Ther* 2001;8:89–98.
- Barker DD, Berk AJ. Adenovirus proteins from both E1B reading frames are required for transformation of rodent cells by viral infection and DNA transfection. *Virology* 1987;156:107–121.
- Nemunaitis J, Ganly I, Khuri F, Arseneau J, Kuhn J et al. Selective replication and oncolysis in p53 mutant tumors with ONYX-015, an E1B-55kD gene-deleted adenovirus, in patients with advanced head and neck cancer: a phase II trial. *Cancer Res* 2000;60:6359–6366.
- Goodrum FD, Ornelles DA. p53 status does not determine outcome of E1B 55-kilodalton mutant adenovirus lytic infection. *J Virol* 1998;72:9479–9490.
- Harada JN, Berk AJ. p53-Independent and -dependent requirements for E1B-55K in adenovirus type 5 replication. *J Virol* 1999;73:5333–5344.
- Turnell AS, Grand RJ, Gallimore PH. The replicative capacities of large E1B-null group A and group C adenoviruses are independent of host cell p53 status. *J Virol* 1999;73:2074–2083.
- O'Shea CC, Johnson L, Bagus B, Choi S, Nicholas C et al. Late viral RNA export, rather than p53 inactivation, determines ONYX-015 tumor selectivity. *Cancer Cell* 2004;6:611–623.
- Woo JL, Berk AJ. Adenovirus ubiquitin-protein ligase stimulates viral late mRNA nuclear export. *J Virol* 2007;81:575–587.
- Blanchette P, Kindsmüller K, Groitl P, Dallaire F, Speiseder T et al. Control of mRNA export by adenovirus E4orf6 and E1B55K proteins during productive infection requires E4orf6 ubiquitin ligase activity. *J Virol* 2008;82:2642–2651.
- Aoki W, Tatsukami Y, Kitahara N, Matsui K, Morisaka H et al. Elucidation of potentially virulent factors of *Candida albicans* during serum adaptation by using quantitative time-course proteomics. *J Proteomics* 2013;91:417–429.
- Matheson NJ, Sumner J, Wals K, Rapiteanu R, Weekes MP et al. Cell surface proteomic map of HIV infection reveals antagonism of amino acid metabolism by Vpu and Nef. *Cell Host Microbe* 2015;18:409–423.
- Evans VC, Barker G, Heesom KJ, Fan J, Bessant C et al. De novo derivation of proteomes from transcriptomes for transcript and protein identification. *Nat Methods* 2012;9:1207–1211.
- Chahal JS, Gallagher C, DeHart CJ, Flint SJ. The repression domain of the E1B 55-kilodalton protein participates in countering interferon-induced inhibition of adenovirus replication. *J Virol* 2013;87:4432–4444.

38. Wright J, Leppard KN. The human adenovirus 5 L4 promoter is activated by cellular stress response protein p53. *J Virol* 2013;87:11617–11625.
39. Croft D, Mundo AF, Haw R, Milacic M, Weiser J et al. The reactome pathway knowledgebase. *Nucleic Acids Res* 2014;42:D472–D477.
40. Fabregat A, Sidiropoulos K, Garapati P, Gillespie M, Hausmann K et al. The reactome pathway knowledgebase. *Nucleic Acids Res* 2016;44:D481–D487.
41. Blackford AN, Grand RJ. Adenovirus E1B 55-kilodalton protein: multiple roles in viral infection and cell transformation. *J Virol* 2009;83:4000–4012.
42. Ikeda K, Quertermous T. Molecular isolation and characterization of a soluble isoform of activated leukocyte cell adhesion molecule that modulates endothelial cell function. *J Biol Chem* 2004;279:55315–55323.
43. Iolyeva M, Karaman S, Willrodt AH, Weingartner S, Vigl B et al. Novel role for ALCAM in lymphatic network formation and function. *FASEB J* 2013;27:978–990.
44. Bartee E, McCormack A, Früh K. Quantitative membrane proteomics reveals new cellular targets of viral immune modulators. *PLoS Pathog* 2006;2:e107.
45. Zantek ND, Azimi M, Fedor-Chaiken M, Wang B, Brackenbury R et al. E-cadherin regulates the function of the EphA2 receptor tyrosine kinase. *Cell Growth Differ* 1999;10:629–638.
46. Lee H, Bennett AM. Receptor protein tyrosine phosphatase-receptor tyrosine kinase substrate screen identifies EphA2 as a target for LAR in cell migration. *Mol Cell Biol* 2013;33:1430–1441.
47. Makarov A, Ylivinkka I, Nyman TA, Hyytiäinen M, Keski-Oja J. Ephrin-As, Eph receptors and integrin  $\alpha 3$  interact and colocalise at membrane protrusions of U251MG glioblastoma cells. *Cell Biol Int* 2013;37:1080–1088.
48. Matthews DA, Russell WC. Adenovirus protein-protein interactions: hexon and protein VI. *J Gen Virol* 1994;75:3365–3374.
49. Kanegae Y, Makimura M, Saito I. A simple and efficient method for purification of infectious recombinant adenovirus. *Jpn J Med Sci Biol* 1994;47:157–166.
50. Blanchette P, Cheng CY, Yan Q, Ketner G, Ornelles DA et al. Both BC-box motifs of adenovirus protein E4orf6 are required to efficiently assemble an E3 ligase complex that degrades p53. *Mol Cell Biol* 2004;24:9619–9629.
51. Sarnow P, Sullivan CA, Levine AJ. A monoclonal antibody detecting the adenovirus type 5-E1b-58Kd tumor antigen: characterization of the E1b-58Kd tumor antigen in adenovirus-infected and -transformed cells. *Virology* 1982;120:510–517.

### Five reasons to publish your next article with a Microbiology Society journal

1. The Microbiology Society is a not-for-profit organization.
2. We offer fast and rigorous peer review – average time to first decision is 4–6 weeks.
3. Our journals have a global readership with subscriptions held in research institutions around the world.
4. 80% of our authors rate our submission process as 'excellent' or 'very good'.
5. Your article will be published on an interactive journal platform with advanced metrics.

Find out more and submit your article at [microbiologyresearch.org](http://microbiologyresearch.org).